International Journal on
"Technical and Physical Problems of Engineering"
(IJTPE)
Published by International Organization of IOTPE

ISSN 2077-3528
IJTPE Journal
www.iotpe.com
ijtpe@iotpe.com

September 2022 | Issue 52 | Volume 14 | Number 3 | Pages 36-43

DESIGN OF A VSC-BASED STATCOM EQUIPPED WITH AN OPEN LOOP CURRENT CONTROLLER

A.M. Obais

Department of Biomedical Engineering, University of Babylon, Babylon, Iraq, eng.abdul.kareem@uobabylon.edu.iq

Abstract- In this paper, a single phase STATCOM constructed of a voltage source converter (VSC) is introduced. The STATCOM DC capacitor is shunted by a harmonic filtering circuit for smoothing its voltage profile. The current of the devised STATCOM is controlled via a new controller addressing the STATCOM voltage angle in the range of $\pm 5.7^0$ with respect to the AC input phase voltage. This small range of angle control makes the STATCOM offer linear and continuous response to pure reactive current demand without association of harmonics or exchange of active power with the AC source. This STATCOM is designed and tested on PSpice. The simulation results of this STATCOM have verified its design methodology.

Keywords: Energy Saving, Harmonics, Power Quality, STATCOM, Static VAR Compensator, VAR.

1. INTRODUCTION

Static VAR compensators SVCs help to save energy, keep constant AC voltage profile, control the parameters of the AC power systems for the purposes of power stability, and reduce losses of transmission lines in order to operate them closer their maximum ratings. SVCs are very essential in power system networks due to their exploitations in applications requiring exchange of VAR and real power with the AC grid. The exchange processes with the AC networks are usually accomplished via small reactors. Such processes rather cause injection of spreading spectrums of harmonic currents revealing in the AC source side [1]. Many works were conducted to decrease the effects of these current harmonics associating such SVCs. Multilevel technology was employed in [2] for generating to some extent sinusoidal voltage from an inverter used in these compensators.

In [3], a power converter based static compensator was built of cascaded H-bridges and provided with a control strategy for balancing the DC-BUS voltage and solving the balancing problems via keeping equally distributed VAR among all the H-bridges of the devised converter. Despites the load might absorb reactive and harmonic currents from the AC grid, an active power filter was suggested by [4] to be capable of balancing the AC current fundamental at unity power factor. A STATCOM in [5] was linearized around a certain point of operation via a model based on a set linearized nonlinear equation. Using a triangular carrier switching strategy, a 2-level inverter governed by phase-shifted multicarrier unipolar pulse width modulation was proposed by [6]. This control scheme was feasible to be extended for cascaded multilevel converters.

A synthesized arrangement of multilevel inverters was built in [7] using multiples of single and 3-phase schemes. This arrangement leads to the construction of converters having higher voltage levels. An equivalent 3-phase, star-connected AC supply was attached to a STATCOM, which was required to be conditioned such that zero average active power can be produced in each phase under unbalanced supply voltages or unbalanced compensating currents [8].

A reduced-rating voltage-source inverter-based SVC was proposed by [9] in a 3-phase 4-wire system. This SVC was attached to a zig-zag distribution transformer to construct a DSTATCOM, which was employed to accomplish power-quality improvement including harmonics cancellation, load balancing, VAR compensation, and voltage compensation at point of common coupling. To accomplish better operation in AC power systems with unbalanced and distorted medium-voltage characterized by large-currents, a transformer less four-leg STATCOM devised from cascaded half-bridge converters was proposed by [10], while for voltage and current compensation in [11], Instantaneous Power Theory was employed for real-time computation and control for a 3-phase STATCOM. A STATCOM was devised in [12] to govern the exciter of an induction generator. A synthetic algorithm was adopted in this work to specify four controllers for dc voltage, ac voltage, ac reactive current, and ac active current. With suitable design of eigen structure in the STATCOM state variables, reactive and active currents were driven using new respective modes.

An experimental model of FACTS designed on the basis of VSC topology was introduced by [13]. The model provided an effective solution to poor power quality and the problem of AC to DC power transformation requirements in power system networks. The design considerations of the DC capacitor and the coupling inductor of the STATCOM in power system networks were analyzed in [14]. Amplitude and phase control schemes were employed as a basic control strategy for the STATCOM starting from modelling the STATCOM

system through frequency domain and ending with the effects of the DC side capacitor and coupling inductor on the filtering characteristics and the stability of the STATCOM.

The work introduced by [15] studied different control schemes concerning DSTATCOMs, which are intended to solve various power quality problems in distribution power systems. A computer simulation was carried out in [16] on a STATCOM connected in delta form using a multilevel converter built of cascaded H-bridges. The STATCOM was exploited for power factor correction and load balancing of unbalanced three-phase load in a distribution network. Feed-forward compensation equations were derived for the STATCOM using the method of symmetrical components.

A work in [17] presented a comprehensive methodology to obtain the support of the VAR capability and its associated costs concerning single- and two-stages PV farms throughout the operation of daytime. Results verified that the employment of two-stage PV farms was capable of expanding the VAR support capability for low irradiances compared to single-stage PV farms. An analysis modality on the basis of the theory of magnitude-phase dynamic for STATCOMs in isolated power systems was introduced by [18]. In this work, the stability margin was greatly decreased when a load was connected to an isolated power system due to the disadvantages of the self-excited induction generators.

The planning framework of a distribution system related to the flexible electric vehicle loads was discussed in [19]. The hosting capability of the electric vehicle loads on distribution networks was enhanced for maintaining better power quality, which was a pre-requisite for increasing the engagement of the power consumers. A phase angle of a single-phase STATCOM was modeled according to its structure in [20] to address the unknown external disturbances and its dynamics, so that the external disturbances and modeling uncertainties can be realized without using approximations for functions.

A work in [21] introduced the employment of STATCOMs in VAR compensation to enhance the capability of the Fault Ride-Through and accomplish improvement to the dynamic performance of power systems attached to PV/wind hybrid during the transient disturbances of the grid. A STATCOM is imperative to accomplish constant voltage stability at the transmission line ends. The mechanisms of VSC schemes with the methodologies of switching frequency control are broadly used to achieve VAR compensation [22]. The performance of a STATCOM and Double Fed Induction Generator (DFIG) in a transmission system was studied by [23]. The speed of induction generator rotor is always changing in a nonlinear manner with respect to wind speed. Under such a situation, the system performance is disturbed.

The integration of the DFIG and the STATCOM system can stabilize the profile of the system voltage and enhance the flexible power flow in a transmission system. A peak-value control of dc voltage is usually proposed for supporting the use of a smaller dc capacitance for single-phase VSC-based STATCOM.

Although such a kind of control was verified to operate in a stable manner under many conditions, [24] revealed that this control strategy will suffer from severe small-signal stability issues under non-ideal system conditions than the traditional methods represented by controlling the average dc voltage.

A two-stage converter built of single-phase H-bridge and a DC-DC converter was dedicated in [25] for PV applications purposed due its high voltage gain characteristics. This configuration is characterized by minimized switches voltage stresses on the DC-DC side. A three-phase VSC having twelve switching devices and equipped with hysteresis band controller was proposed in [26] for voltage control and harmonic minimization. The proposed topology converter had rapid transient response toward voltage distortion.

In this paper, a single-phase harmonic-free linearly controlled voltage source converter based STATCOM equipped with an open loop current controller is introduced. The STATCOM is built of an H-bridge voltage source converter loaded by a DC capacitor equipped with a smoothing harmonic filtering circuit and exchanges reactive power with the AC source via harmonic suppressing reactor. The STATCOM current controller is designed on the basis of open loop control of the STATCOM angle in a preassigned linear region of operation.

2. THE PROPOSED STATCOM

Figure 1 shows the proposed STATCOM. It is built of a full H-bridge voltage source converter having a composite DC link and a series reactor to exchange VAR with the AC source. The series reactor is represented by the series combination $L_S R_S$, where L_S is its self-inductance and R_S is its self-resistance. The DC link is built of a DC capacitor C_{DC} and filtering circuit represented by L_{DCF}, C_{DCF}, and R_{DCF} to smoothen the DC voltage profile of C_{DC}. R_{DCF} represents the self-resistance of the reactor L_{DCF}. The filtering circuit resonates at twice the AC source frequency f.

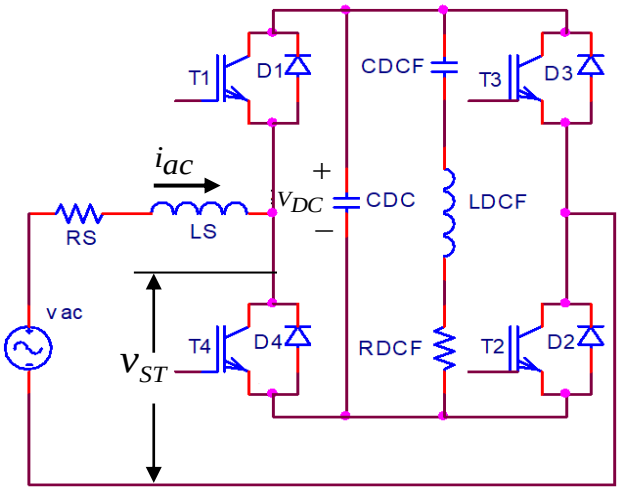

Figure 1. Power circuit of the proposed STATCOM

The voltage source converter is driven by the insulated gate bipolar transistors IGBTs, which are T_1, T_2, T_3, and T_4. These IGBTs are provided with D_1, D_2, D_3, and D_4 the as diodes for free-wheeling purposes and controlled using SPWM. The triggering mechanism of the IGBTs T_1 and T_3 is shown in Figure 2. The triangular waveform v_{TRI} represents the carrier signal of SPWM and v_{MD} represents its modulating signal. The modulating signal v_{MD} is a sinusoidal analog voltage running at the same AC supply frequency f of the voltage v_{ac} and shifted from it by a small angle β. Where, β is the STATCOM angle and varies in a linear region of ±0.1 rad. $+A_{TRI}$ represents the amplitude or the maximum level of v_{TRI}, while $-A_{TRI}$ represents its maximum negative level. The carrier signal v_{TRI} is running at a carrier frequency f_{TRI}, which should be very much greater than the AC source frequency f, which represents the running frequency of the modulating signal v_{MD}. V_{T1} and V_{T3} are the triggering signals of the IGBTs T_1 and T_3, respectively. The voltage v_{ST} represents the H-bridge input voltage, which is directly proportional to the capacitor DC voltage V_{DC}. ω is the AC source angular frequency and is equal to $2\pi f$.

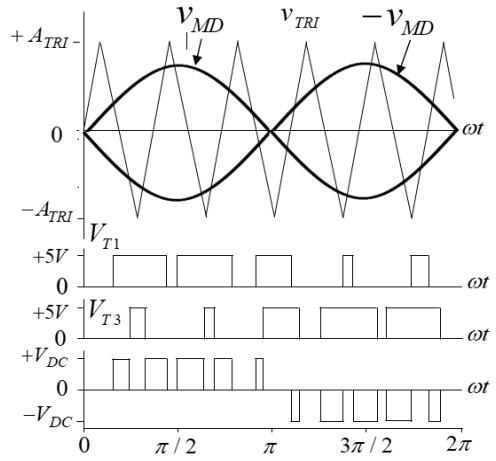

Figure 2. The STATCOM sinusoidal pulse width modulation

According to Figure 2, if V_{DC} is kept constant then v_{ST} will be given by

$$v_{ST} = V_{DC}\left(\frac{V_{T1} - V_{T3}}{5}\right) \tag{1}$$

where, the number 5 in the above equation stands for the maximum positive level of the triggering signals V_{T1} and V_{T3}. The modulating signal v_{MD} can be expressed by

$$v_{MD} = A_{MD}\sin(\omega t - \beta) \tag{2}$$

where, A_{MD} is the amplitude of v_{MD}. Figure 3 shows the generated voltage v_{ST} of the H-bridge VSC during a certain one cycle of v_{TRI}. In this figure, the carrier signal frequency f_{TRI} is very much greater than the modulating signal frequency f. For a certain value of m, v_{ST} average throughout v_{TRI} one cycle duration T_{TRI} is referred to as v_{STa}, which can be given by

$$v_{STa} = \frac{1}{T_{TRI}}\left(\int_{t'_1}^{t'_2} V_{DC}\,dt' + \int_{t'_3}^{t'_4} V_{DC}\,dt'\right) = mV_{DC}\sin(\omega t - \beta) \tag{3}$$

where, m is modulation index and it is defined by

$$m = \frac{A_{MD}}{A_{TRI}} \tag{4}$$

To make Equation (4) applicable over the carrier signal profile, kT_{TRI} is substituted for t and $2\pi/T$ for ω. Where, T is the time duration of the modulating signal and k=1, 2, 3, and so on. Consequently, it can be written

$$v_{STa}\left(\frac{k}{N}\right) = mV_{DC}\sin\left(\frac{2\pi}{T_{MD}}kT_{TRI} - \beta\right) = mV_{DC}\sin\left(\frac{2\pi}{N}k - \beta\right) \tag{5}$$

where, the number N is given by

$$N = \frac{T}{T_{TRI}} \tag{6}$$

The voltage v_{STa} shows sinusoidal profile in phase with v_{MD} during its variation with ωt. This implies that the average voltage profile of v_{ST} shows a fundamental voltage referred to as v_{ST1}, which can be expressed by

$$v_{ST1} = mV_{DC}\sin(\omega t - \beta) \tag{7}$$

Supposing that the series reactor of the STATCOM eliminates all the components of the harmonics, then the STATCOM r.m.s current fundamental I_{ac} is expressed by

$$Iac = \frac{V_{A.C} - V_{ST1}\angle(-\beta)}{R_S + j\omega L_S} \approx \frac{V_{A.C} - V_{ST1}\angle(-\beta)}{j\omega L_S},\ |\omega L_S|^2 >> |R_S|^2 \tag{8}$$

where, V_{AC} is the r.m.s of v_{ac} and V_{ST1} is the r.m.s of v_{ST1}. V_{ST1} can be defined by

$$V_{ST1} = mV_{DC}/\sqrt{2} \tag{9}$$

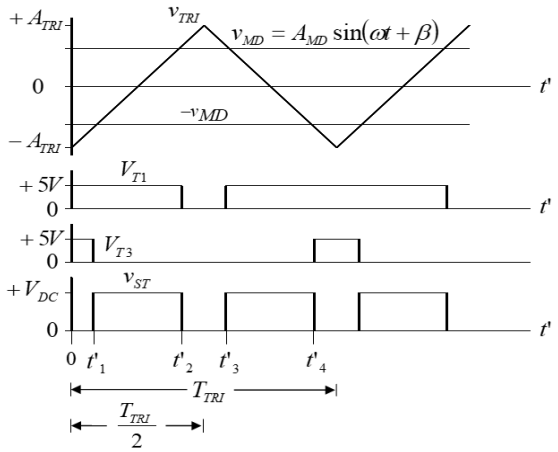

Figure 3. The generated voltage v_s within one cycle of v_{TRI}

For small values of β, If V_{ST1} is greater than V_{AC}, I_{ac} will be capacitive and will be inductive if V_{ST1} is less than V_{AC}.

2.1. The Devised Open Loop STATCOM Controller

The proposed STATCOM is designed to operate at an AC source having a frequency f of 50 Hz. The duration time of one cycle is 20 ms. Figure 4 shows the schematic design of the devised open loop current controller of the proposed STATCOM. Two parts are forming this controller. The first part is represented by the STATCOM angle controller, whereas the second part is its triggering circuit. The input to the angle controller is the two analog voltage signals k_1v_{ac}=$k_1$311sinωt=5sinωt and k_2I_{RD}. Where, k_1 is a reduction factor stands for 0.016, I_{RD} is the reactive current demand, and k_2 is a reduction factor stands for 0.05 V/A. the analog voltage k_2I_{RD} is a DC signal voltage varying in the range of ±5 V for a reactive current demand I_{RD} varying in the range of ±100 A (peak value). The inputs to the analog multiplier are the two analog inputs v_1 and v_2, which are given by

$$v_1 = 5\sin\left(\omega t - \frac{\pi}{2}\right) \tag{10}$$

$$v_2 = k_2 I_{RD} \tag{11}$$

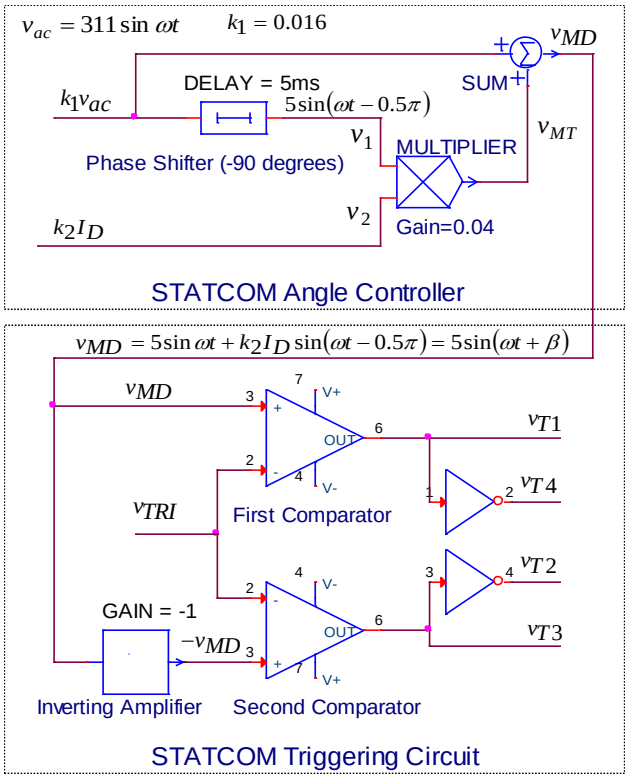

Figure 4. The STATCOM open loop current controller

The analog multiplier output voltage v_{MT} can be expressed by;

$$v_{MT} = A_{MT}v_1v_2 = 5\sin\left(\omega t - \frac{\pi}{2}\right)k_2I_{RD}A_{MT} \tag{12}$$

where, A_{MT} corresponds to the analogue multiplier gain and is equal to 0.04. Note that v_1 represents the analog voltage k_1v_{ac} delayed by 5 ms or shifted by angle of -π/2. The term $k_2I_{RD}A_{MT}$ in the output of the multiplier v_{MT} is varying in the range of ±0.1 V. The output of the summer is the modulating signal v_{MD}, which can be given by

$$v_{MD} = k_1v_{ac} + v_{MT} =$$

$$= 0.016\times311\sin(\omega t) + 5\sin\left(\omega t - \frac{\pi}{2}\right)k_2I_{RD}A_{MT} = \tag{13}$$

$$= 5\left(\sqrt{\left(k_2I_{RD}A_{MT}\right)^2 + 1}\right)\sin\left(\omega t - \tan^{-1}(\beta)\right)$$

where, β is the STATCOM angle, which can be given by

$$\beta = k_2I_{RD}A_{MT} \tag{14}$$

Since, the controller is designed such that the term $k_2I_{RD}A_{MT}$ is varying in the range of ±0.1 V according to I_{RD}, then tan^{-1}(β) can be approximated to β and Equation (13) can be rewritten as

$$v_{MD} = 5\sin(\omega t - \beta) \tag{15}$$

By varying β from -0.1 rad to +0.1 rad, the fundamental STATCOM voltage V_{ST1} varies from minimum to maximum. Positive values of β of correspond to capacitive currents, whereas negative values correspond to inductive currents. V_{T1} is obtained by comparing v_{MD} with v_{TRI} and V_{T3} is obtained by comparing -v_{MD} with v_{TRI}.

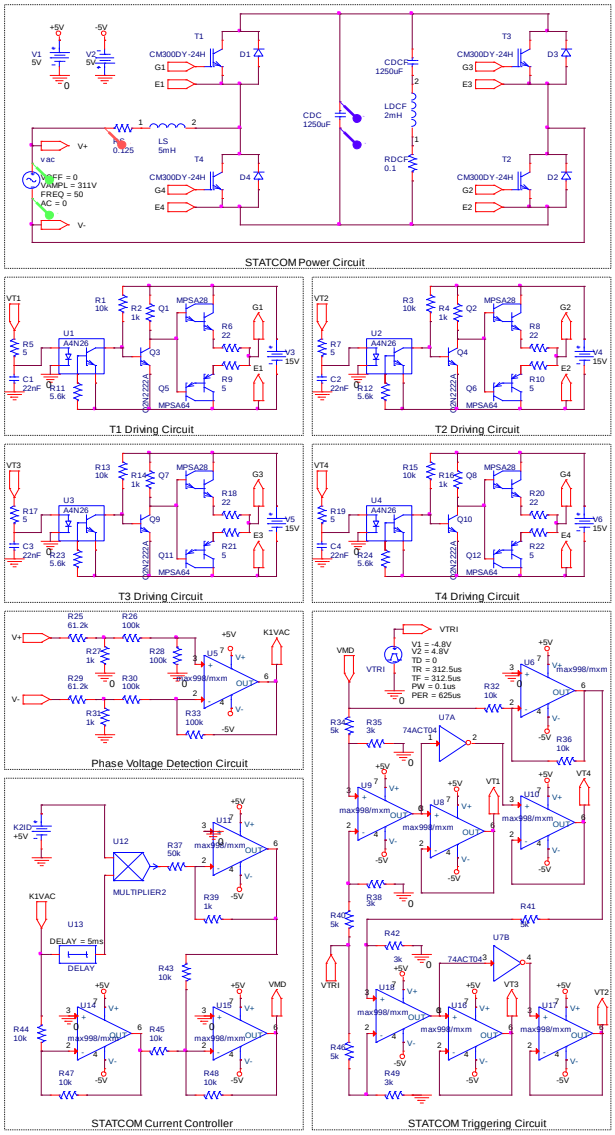

Figure 5. The STATCOM proposed PSpice design

2.2. The STATCOM Circuit Design

Figure 5 shows the circuit design corresponding to the proposed STATCOM, is driven by 220 Vr.m.s (311 V peak value), 50 Hz AC voltage. The proposed STATCOM is designed to respond to maximum capacitive current demand of 100 A as a peak and a maximum inductive reactive current demand of -100 A (peak value). Here the (-) sign refers to inductive currents.

This STATCOM is designed on PSpice, which is very close in performance to real hardware. The IGBTs used are type CM300DY-24H. This IGBT has 1200 V as a maximum voltage rating and 300 A as a maximum current rating. In addition, it is capable of handling a power dissipation of 2100 W. The value of the STATCOM reactor L_S is chosen such that the STATCOM is capable of satisfying a maximum reactive current (capacitive or inductive) of |100| A (peak value) when $|\beta|$=0.1 rad. The carrier signal v_{TRI} has a frequency f_{TRI} of 1.6 kHz. The DC capacitor filtering circuit is designed such the 100 Hz harmonic component of V_{DC} is significantly reduced.

3. SIMULATION RESULTS

The STATCOM circuit shown in Figure 5 was tested on PSpice for investigating its reactive current responses to current demands varying from maximum pure inductive current of -100 A (peak value) to maximum capacitive current of +100 A (peak value). Figure 6 reveals the response of the STATCOM to current demand of -100 A (peak value), which represents the maximum inductive that can be supplied by the STATCOM. Figure 6a shows the transient instantaneous AC voltage v_{ac}, STATCOM current i_{ac}, and the DC capacitor voltage V_{DC}, while Figure 6b shows their steady state responses. This inductive current demand corresponds to a controlling voltage k_2I_{RD} of a value of -5 V.

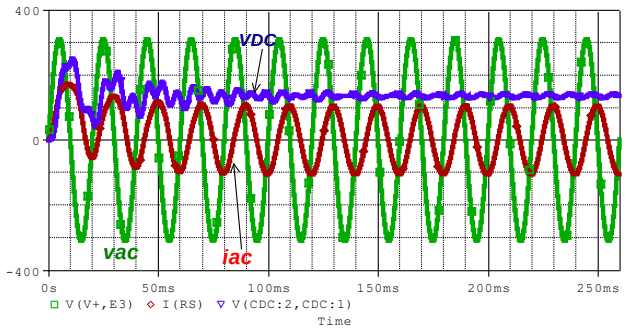

(a)

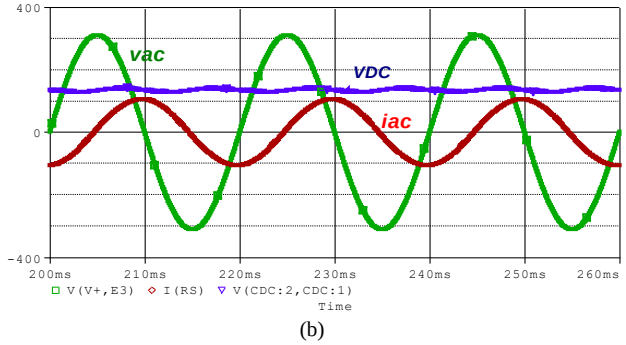

(b)

Figure 6. The STATCOM inductive response to a current demand of -100 A as a peak, (a) transient response and (b) steady state response

It is obvious that the STATCOM approaches its steady state within five cycles of the AC input phase voltage and the STATCOM current is really -100 A peak value. Here the minus sign is used to distinguish between the STATCOM capacitive current, which leads the AC input voltage by an angle of $\pi/2$ and the inductive current, which lags v_{ac} by an angle of $\pi/2$.

The STATCOM inductive response to a current demand of -50 A (peak value) is shown in Figure 7. Here the amount of reactive current demand in this figure corresponds to k_2I_{RD} of -2.5 V. Again, Figure 7 verifies that the STATCOM approaches its steady state within five cycles of v_{ac} and its actual current satisfies the reactive current demand.

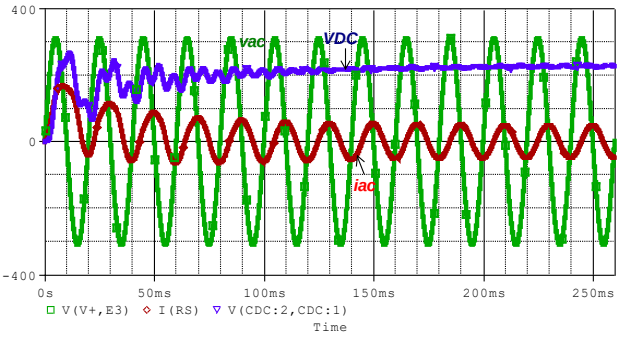

(a)

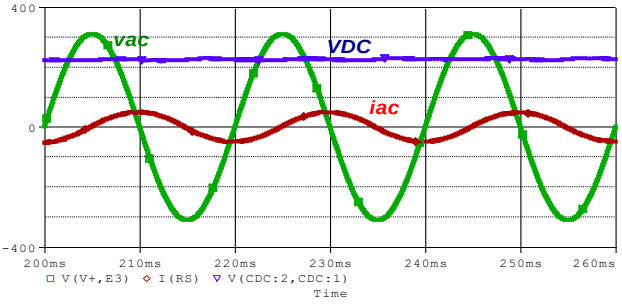

(b)

Figure 7. The STATCOM inductive response to a current demand of -50 A as a peak, (a) transient response and (b) steady state response

Figure 8 shows the STATCOM performance during a current demand of zero value. In this test, the controlling analog voltage k_2I_{RD} has a value of 0 V.

Both Figures 6 and 7 state that the STATCOM current lags the AC voltage by an angle of $\pi/2$ and that verifies its pure inductive reactive current response, while Figure 8 verifies its zero reactive current response to a current demand of zero value. The STATCOM capacitive response to a demand current of +50 A (peak value) is shown in Figure 9. The current demand in this figure corresponds to k_2I_{RD} of +2.5 V. It is obvious that the STATCOM current leads the input AC voltage by an angle of $\pi/2$, which verifies the pure capacitive reactive current response to a current demand of +50 A (peak value). The STATCOM performance during its response to capacitive reactive elapses more time in order to approach its steady state response. This is due to fact that certifies inductive initiation of STATCOM current, since the DC capacitor voltage always starts from zero and then grows up gradually to its steady state value.

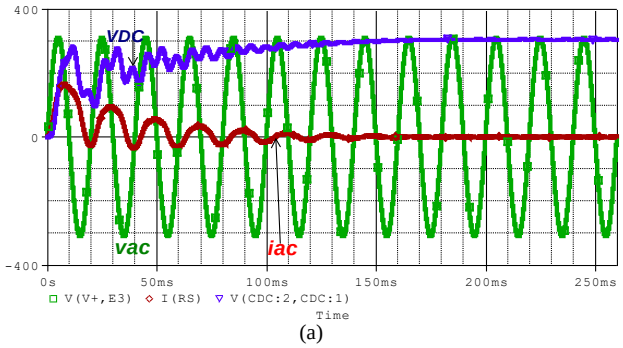

(a)

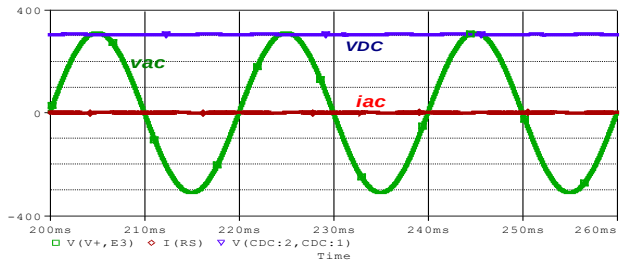

(b)

Figure 8. The STATCOM performance during zero reactive current demand, (a) transient response and (b) steady state response

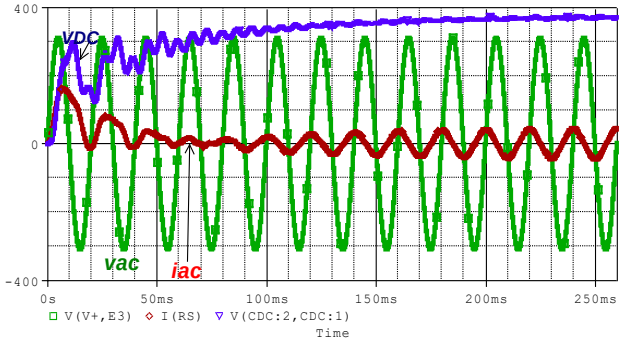

(b)

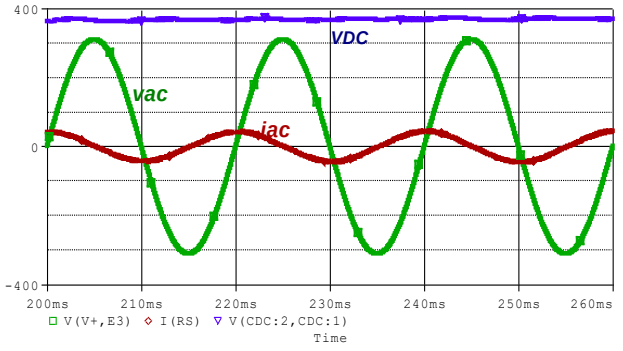

(b)

Figure 9. The STATCOM response capacitive to a current demand of 50 A as a peak, (a) transient response and (b) steady state response

Figure 10 shows the STATCOM response to a maximum capacitive current demand of +100 A as a peak. This capacitive current demand corresponds to $k_2 I_{RD}$ of +5 V. It is obvious that the STATCOM current is really +100 A peak value, which complies with the required capacitive reactive current demand. Similarly, Figure 10 demonstrates that the STATCOM elapses more time throughout its settlement to state operation. In all of the above tests, the STATCOM angle β remains within the preassigned range, which is limited to ±1 rad.

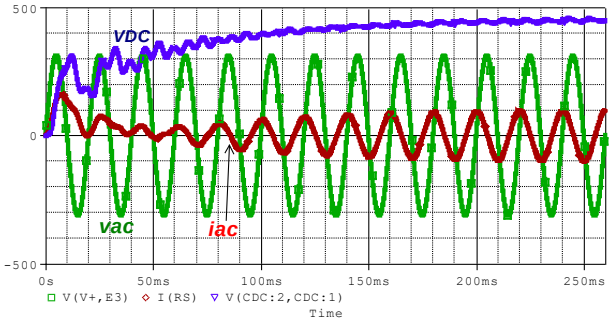

(a)

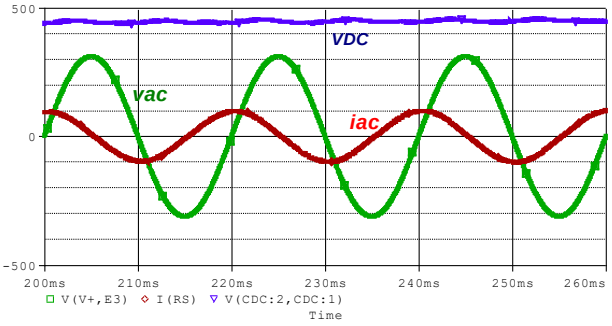

(b)

Figure 10. The STATCOM capacitive response to a current demand of 100 A as a peak, (a) transient response and (b) steady state response

Figure 11 shows the STATCOM current variation against current demand. The figure shows high linearity and this is due to almost linear relationship of $\tan^{-1}(\beta)$ with respect to β within the preassigned range of operation. As all inductive and capacitive reactive current responses exhibit pure and harmonic free reactive currents throughout STATCOM operation in steady state regions, the proposed STATCOM is promoted as linearly controlled pure reactive element in both capacitive and inductive operation modes.

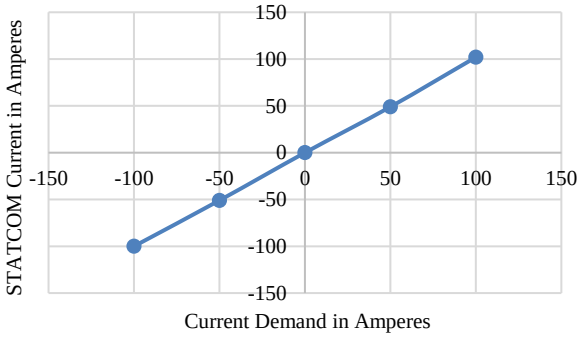

Figure 11. STATCOM Current variations with current demand

4. CONCLUSIONS

In this work, a harmonic-free and linearly controlled STATCOM is introduced. It is feasible to be employed in applications requiring continuously controlled pure reactive elements characterized by high linearity and negligible harmonic associations. Thus, this STATCOM is promoted as an adaptively controlled compensating susceptance in power quality applications like load current balancing and voltage control.

NOMENCLATURES

1. Acronyms

DFIG	Double Fed Induction Generator
DSTATCOM	Distribution STATCOM
IGBT	Insulated gate bipolar transistor
PV	Photovoltaic
SPWM	Sinusoidal Pulse Width Modulation
STATCOM	Static compensator
SVC	Static VAR compensator
VAR	Reactive power
VSC	Voltage source converter

2. Symbols / Parameters

A_{MD} : The amplitude of the modulating signal

A_{MT} : Multiplier gain

A_{TRI} : The triangular voltage amplitude

β : The STATCOM angle

C_{DC} : The DC capacitor

f : The AC source frequency

f_{TRI} : The triangular voltage frequency

i_{ac} : The STATCOM AC current

I_{RD} : The reactive current demand

k : A number equal to 1, 2, 3, …

k_1, k_2 : Constants

L_S : The STATCOM reactor

m : The modulation indexes

N : The time duration ratio of modulating to carrier signals

R_S : The self-resistance of STATCOM reactor

t : Time

T_{MD}, T : Duration time of modulating signal

T_{TRI} : Duration time of carrier signal

v_1, v_2 : Multiplier input signals

v_{ac} : The AC phase voltage

V_{DC} : The DC capacitor voltage

v_{MD} : The modulating signals

v_{MT} : Multiplier output voltage

v_{ST} : The H-bridge or STATCOM input voltage

V_{ST1} : The STATCOM fundamental voltage

v_{STa} : The STATCOM average input voltage

V_{T1} : The triggering signal of the IGBT T_1

V_{T2} : The triggering signal of the IGBT T_2

V_{T3} : The triggering signal of the IGBT T_3

V_{T4} : The triggering signal of the IGBT T_4

v_{TRI} : The triangular voltage

ω : The AC source angular frequency

REFERENCES

[1] R. Sternberger, D. Jovcic, "Theoretical Framework for Minimizing Converter Losses and Harmonics in a Multilevel STATCOM", IEEE Transactions on Power Delivery, Vol. 23, No. 4, pp. 2376-2384, 2008.

[2] H.P. Mohammadi, M.T. Bina, "A Transformerless Medium-Voltage STATCOM Topology Based on Extended Modular Multilevel Converters", IEEE Transactions on Power Electronics, Vol. 26, No. 5, pp. 1534-1545, 2011.

[3] J.A. Barrena, L. Marroyo, M.A.R. Vidal, J.R.T. Apraiz, "Individual Voltage Balancing Strategy for PWM Cascaded H-Bridge Converter-Based STATCOM", IEEE Transactions on Industrial Electronics, Vol. 55, No. 1, pp. 21-29, 2008.

[4] S. Hirve, K. Chatterjee, B.G. Fernandes, M. Imayavaramban, S. Drawi, "PLL-Less Active Power Filter Based on One-Cycle Control for Compensating Unbalanced Loads in Three-Phase Four-Wire System", IEEE Transaction on Power Delivery, Vol. 22, No. 4, pp. 2457-2465, 2007.

[5] Y. Ye, M. Kazerani, V.H. Quintana, "Current-Source Converter Based STATCOM: Modeling and Control", IEEE Transaction on Power Delivery, Vol. 20, No. 2, pp. 795-800, 2005.

[6] R. Gupta, A. Ghosh, A. Joshi, "Switching Characterization of Cascaded Multilevel Inverter Controlled Systems", IEEE Transactions on Industrial Electronics, Vol. 55, No. 3, pp. 1047-1058, 2008.

[7] J. Wen, K.M. Smedley, "Synthesis of Multilevel Converters Based on Single and or Three-Phase Converter Building Blocks", IEEE Transactions on Power Electronics, Vol. 23, No. 3, pp. 1247-1256, 2008.

[8] Q. Song, W. Liu, "Control of a Cascade STATCOM with Star Configuration under Unbalanced Conditions", IEEE Transactions on Power Electronics, Vol. 24, No. 1, pp. 45-58, 2009.

[9] B. Singh, P. Jayaprakash, T.R. Somayajulu, D.P. Kothari, "Reduced Rating VSC with a Zig-Zag Transformer for Current Compensation in a Three-Phase Four-Wire Distribution System", IEEE Transaction on Power Delivery, Vol. 24, No. 1, pp. 249-259, 2009.

[10] H.P. Mohammadi, M.T. Bina, "A Transformer less Medium-Voltage STATCOM Topology Based on Extended Modular Multilevel Converters", IEEE Transactions on Power Electronics, Vol. 26, No. 5, pp. 1534-1545, 2011.

[11] Y. Xu, L. M. Tolbert, J.D. Kuek, D.T. Rizy, "Voltage and Current Unbalance Compensation Using a Static Var Compensator", IET Power Electronics, Vol. 3, No. 6, pp. 977-988, 2010.

[12] W.L. Chen, W.G. Liang, H.S. Gau, "Design of a Mode Decoupling STATCOM for Voltage Control of Wind-Driven Induction Generator Systems", IEEE Transactions on Power Delivery, Vol. 25, No. 3, pp. 1758-1767, 2010.

[13] S.K. Umathe, K.D. Joshi, "STATCOM: Theoretical Aspects & Experimental Study", International Journal of Electrical Engineering, Vol. 4, No. 4, pp. 439-448, 2011.

[14] G. Zhao, M. Han, J. Liu, "Analysis and Design of the Interface Inductor and the DC Side Capacitor in a STATCOM with Phase and Amplitude Control Considering the Stability of the System", Journal of Power Electronics, Vol. 12, No. 1, pp. 193-200, 2012.

[15] G. Gupta1, W. Fritz, M.T.E. Kahn, "A Comprehensive Review of DSTATCOM: Control and Compensation Strategies", International Journal of Applied Engineering Research, Vol. 12, No. 12, pp. 3387-3393, 2017.
[16] W.N. Chang, C.H. Liao, "Design and Implementation of a STATCOM Based on a Multilevel FHB Converter with Delta-Connected Configuration for Unbalanced Load Compensation", Energies, Vol. 10, No. 7, pp. 1-17, 2017.
[17] L.F.N. Lourenço, R.M. Monaro, M.B.C. Salles, J.R. Cardoso, L. Queval, "Evaluation of the Reactive Power Support Capability and Associated Technical Costs of Photovoltaic Farms' Operation", Energies, Vol. 11, No. 6, pp. 1-20, 2018.
[18] H. Wang, X. Wu, R. You, J. Li, "Modeling and Analysis of SEIG-STATCOM Systems Based on the Magnitude-Phase Dynamic Method", Journal of Power Electronics, Vol. 18, No. 3, pp. 944-953, 2018.
[19] A.H. Zaidi1, K. Sunderland, M. Conlon, "Role of Reactive Power (STATCOM) in the Planning of Distribution Network with Higher EV Charging Level", IET Generation, Transmission and Distribution, Vol. 13, No. 7, pp. 951-959, 2019.
[20] C. Guo, L. Zhong, J. Zhao, G. Gao, "Single-Phase Reactive Power Compensation Control for STATCOMs via Unknown System Dynamics Estimation", Mathematical Problems in Engineering, Vol. 2020, No. 15, pp. 1-9, 2020.
[21] I. Hamdan, A.M.A. Ibrahim, O. Noureldeen, "Modified STATCOM Control Strategy for Fault Ride-Through Capability Enhancement of Grid-Connected PV/Wind Hybrid Power System During Voltage Sag", SN Applied Sciences, Vol. 2, No. 3, pp. 1-19, 2020.
[22] L.N. Gadupudia, G.S. Raob, "Recent Advances of STATCOM in Power Transmission Lines; A Review", Turkish Journal of Computer and Mathematics Education, Vol. 12 No. 3, pp. 4621-4626, 2021.
[23] R.R. Hete, S.K. Mishra, R. Dash, A. Ballaji, V. Subburaj, K.J. Reddy, "Analysis of DFIG-STATCOM P2P Control Action Using Simulated Annealing Techniques", Heliyon, Vol. 8, No. 3, pp. 1-15, 2022.
[24] C. Zhang, T. Isobe, J.A. Suul, T. Dragicevic, M. Molinas, "Parametric Stability Assessment of Single-Phase Grid-Tied VSCs Using Peak and Average DC Voltage Control", IEEE Transactions on Industrial Electronics, Vol. 69, No. 3, pp. 2904-2915, 2022.
[25] S.N. Tackie, B.K. Kurehwatira, "Switched Inductor Capacitor Based DC-AC Converter for PV Applications", International Journal on Technical and Physical Problems of Engineering (IJTPE), Issue 50, Vol. 14, No. 1, pp. 238-246, March 2022.
[26] S. Biricik, S.N. Tackie, O.C. Ozerdem, "Voltage Sag and Swell Mitigation Using Hysteresis Band Controlled Three-Phase Twelve Switch Converter Based DVR", International Journal on Technical and Physical Problems of Engineering (IJTPE), Issue 49, Vol. 13, No. 4, pp. 231-237, December 2021.

BIOGRAPHY

Abdulkareem Mokif Obais was born in Iraq in 1960. He received his B.Sc. and M.Sc. degrees in Electrical Engineering from University of Baghdad, Baghdad, Iraq, in 1982 and 1987, respectively. He received his Ph.D. degree in Electrical Engineering from University Tenaga Nasional, Kajang, Malaysia in 2013. He was promoted to Professor at University of Babylon, Babylon, Iraq in April 2008. He is interested in electronic circuit's design and power electronics. He had supervised and examined a number of postgraduate students. He had published many papers in Iraqi academic and international Journals.